1   Foliar nutrient uptake from dust sustains plant nutrition

2   Anton Lokshin[1,2*], Daniel Palchan[2], Elnatan Golan[3], Ran Erel[3], Daniele Andronico[4], and Avner Gross[1]

3   1.   The Department of Environment, Geoinformatics and Urban planning Sciences, Ben Gurion University of the
4   Negev; Beer Sheva, Israel.
5   2.   The Department of Civil Engineering, Ariel University; Ariel, Israel.
6   3.   Institute of Soil, Water and Environmental Sciences, Gilat Research Center, Agricultural Research Organization;
7   Gilat, Israel.
8   4.   Istituto Nazionale di Geofisica e Vulcanologia, Sezione di Catania-Osservatorio Etneo, Rome, Italy.

10   *** Corresponding author:** Lokshinanton@gmail.com

25

26

27

28

29

30

31

32

`

Abstract

Mineral nutrient uptake from soil through the roots is considered the main nutrition pathway for vascular terrestrial plants. Recently, desert dust was discovered as an alternative nutrient source to plants, through direct uptake from dust deposited on their foliage. Here we studied the uptake of nutrients from freshly deposited desert and volcanic dusts by chickpea plants under ambient and future elevated levels of atmospheric CO_2, through the roots and directly through the foliage. We found that within weeks, chickpea plants acquired phosphorus (P) from dust only through foliar uptake under ambient conditions, and P, Iron (Fe) and Nickel (Ni) under elevated CO2 conditions, significantly increasing their growth. Using additional chickpea variety with contrasting leaf properties we have shown that the foliar nutrient uptake pathway from dust is facilitated by leaf surface chemical and physiological traits such as low pH and trichome densities. We analyzed Nd radiogenic isotopes extracted from plant tissues after dust application to assess the contribution of mineral nutrients that were acquired through the foliage. Our results suggest that foliar mineral nutrient uptake from dust is an important pathway, that may play an even bigger role in an elevated CO_2 world.

Keywords: plant nutrition; Nd isotopes; foliage; elevated CO_2

Introduction

Vascular plants obtain carbon (C) from the atmosphere and most of their mineral nutrients mainly from the soil. Hence, it is generally thought that mineral nutrients such as phosphorus (P), potassium (K), iron (Fe), and other macro and micronutrients are acquired predominantly through the plant's roots system (Marschner et al., 1997). Evidence gathered in recent decades demonstrates that the atmosphere is an important source for mineral-nutrients to terrestrial ecosystems via dust deposition (Chadwick et al., 1999; Goll et al., 2023; Gross et al., 2015; Van Langenhove et al., 2020; Okin et al., 2004; Palchan et al., 2018). The concentration of P (and other nutrients) in mineral atmospheric particles such as desert dust and volcanic ash are enriched relative to most soils and are important plant nutrient sources, especially when soil fertility is low or in dusty regions (Arvin et al., 2017; Bauters et al., 2021; Ciriminna et al., 2022; Eger et al., 2013; Gross et al., 2016b). In a montane environment in California, dust P contribution to plants was documented to outpace the contribution from weathering of host bedrock (Arvin et al., 2017). In a recent study we discovered that certain crop plants can gain P directly from the atmospheric dust, via particles that accumulate on their leaves (Gross et al., 2021a; Lokshin et al., 2024b). Over short time scales, foliar uptake was found as the only P uptake pathway from biomass fire ash particles (while the roots played a negligible role (Lokshin et al., 2024a,b). These recent findings highlights the need to better understand the role of the contribution of nutrient uptake from dust through the foliage (i.e., direct foliar nutrient uptake), a process that has been traditionally overlooked and has never been quantified before, even though foliar fertilization has been a well-known agricultural practice for many decades (Fageria et al., 2009; Ishfaq et al., 2022; Bukovac & Wittwer, 1957; Wittwer & Teubner, 1959). Foliar nutrient uptake occurs through two primary pathways: cuticle penetration and stomatal uptake. The cuticle, while largely hydrophobic, contains aqueous pathways that allow the diffusion of small, polar molecules, particularly under high humidity conditions (Schonherr, 2006). Stomata, which regulate gas exchange, can also act as entry points for hydrophilic solutes and small particles when they are open (Fernández and Eichert, 2009). These pathways can expand or contract dynamically in response to environmental factors, enabling at times solute penetration. Minerals are solid nutrient particles hence need to partially dissolve into the aqueous film on the leaf surface before uptake by the plant. This dissolution can be facilitated by surface moisture, leaf exudates, and microbial activity in the phyllosphere, which enhances the solubility and bioavailability of nutrients (Burkhardt et al., 2012; Fernández et al., 2014, Marschner, 2022).

In the context of climate change, the foliar pathway may be even more pronounced for plants that will grow under elevated CO_2 (eCO_2) conditions because of two documented phenomena: the 'dilution' effect, where accumulation of C exceeds that of mineral nutrients which can lead to stochiometric imbalance (Loladze, 2014), and partial inhibition of key root uptake mechanisms (Gojon et al., 2023), together with soil fertility degradation (Lal, 2009; St. Clair and Lynch, 2010). These changes may lead to the selection of plant traits that facilitate alternative nutrient uptake pathways. The use of the foliar pathway under eCO_2 may offset the alarming phenomenon where an increasing production of carbohydrates causes dilutes the concentration of macro and micronutrients such as P, Fe, calcium (Ca), magnesium (Mg), K, zinc (Zn), copper (Cu), nickel (Ni) and others that are vital for the floral ecological systems (Clarkson and Hanson, 1980).

In this work we designed two experiments to study both the principal mechanisms and biological functions in the plants that benefit foliar nutrient uptake from dust retained on the foliage, and the chemical composition of the

nutrients transferred in this process. Furthermore, we utilized Nd isotopes to attempt quantification of the ion flux from the foliage to the plant. Then we discuss the larger aspect of this newly discovered pathway and its importance.

2 Materials and Methods

2.1 Experimental design

To study the impact of dust deposition on plant nutrition, we selected two contrasting chickpea genotypes (Cicer spp.) from the Hebrew University of Jerusalem chickpea collection. These genotypes were chosen based on previous studies (Gross et al., 2021) that demonstrated differences in their response to foliar dust application. The first genotype, 'CR934,' is a non-responsive genotype of the wild progenitor C. reticulatum, sampled near Savur, Turkey, showing minimal physiological or nutritional changes following dust application. In contrast, the second genotype, 'Zehavit,' is a modern high-yield cultivar widely used by Israeli growers, which exhibits a pronounced response to foliar dust application, such as increase in biomass and total P content. For further biogeochemical analysis of foliar nutrient uptake, the responsive genotype 'Zehavit' was used. Experiments were conducted at Gilat Research Center in southern Israel (31°21' N, 34°42' E) in two separate glasshouse rooms. Temperature was fixed at $25 \pm 3°C$ and relative humidity at 40–50%. Inside the glasshouse the pots were subjected to natural lighting partially concealed by transparent white walls and roof. Overall, the Photosynthetically Active Radiation (PAR) levels were typical for the southern part of Israel during the months of September to November. In one room we set the CO_2 concentration to the ambient 412 ppm (aCO_2) and in the other room to elevated 850 ppm (eCO_2), simulating current and future earth CO_2 concentrations based on high emissions scenario (business as usual, SSP 8.5, IPCC, 2021). Following germination, plants were cultivated in 72 pots containing inert media (perlite 206, particle size of 0.075–1.5 mm; Agrekal, HaBonim, Israel). The pot size was 3 liter, with sufficient room for root growth during the experimental period. All the pots were supplied with a nutrition solution (fertigation) containing the following elements: nitrogen (N) (50 mg L^{-1}), P (3.5 mg L^{-1}), K (50 mg L^{-1}), Ca (40 mg L^{-1}), Mg (10 mg L^{-1}), Fe (0.8 mg L^{-1}), Mn (0.4 mg L^{-1}), Zn (0.2 mg L^{-1}), boron (B) (0.4 mg L^{-1}), Cu (0.3 mg L^{-1}) and molybdenum (Mo) (0.2 mg L^{-1}). The mineral concentrations were achieved by proportionally dissolving NH_4NO_3, KH_2PO_4, KNO_3, $MgSO_4$ and $NaNO_3$. The micronutrients were applied as EDTA (ethylenediaminetetraacetic acid) chelates as commercial liquid fertilizer (Koratin, ICL Ltd). The location of each pot within the glasshouse was randomized at the beginning and changed every two weeks over the course of the experiment. The plants were dripped irrigated 4 times per day for 5 minutes, via an automated irrigation system from the germination stage. At 14 days after germination, when plants were early in the vegetative phase (two or three developed leaves), we changed the nutrient solution of 60 out of the 72 pots to P deficient fertigation (P concentration of 0.1 mg L^{-1}) to create P starvation (-P treatment). Preliminary tests showed that our -P deficient media allows chickpea plants to continue their growth cycle and increase their responsiveness for dust application, reflected in physiological, morphological, and biochemical changes and eCO_2 condition (Gross et al., 2021, Lokshin et al., 2024). The remaining 12 pots continued to receive the full P sufficient nutrient media (+P treatment). Plants fertigated with -P solution started to show P-deficiency symptoms such as chlorosis of mature leaves, slight symptoms of necrotic leaf tips and an overall decrease in biomass accumulation at 35 days after germination. At this stage we applied desert dust and volcanic ash on the -P plants.

`

Of a total number of plants (72) 48 were treated with dust and 24 served as untreated control group. Twenty-four plants were applied with dust on their foliage by manually sprinkling dust through a $63 \mu m$ sieve in proximity to the foliage and 24 plants received root treatment by applying dust through a $63 \mu m$ sieve on the surface of the pot, followed by gentle mixing of the surface to sink the dust particles deeper to enhance the physical contact between the roots and the particles, thereby increasing the chances of having a more significant impact. The experimental design is a 3-factorial design, considering the effects of dust type (desert or volcanic dust), application method (foliar or root), and CO_2 concentration (412 ppm or 850 ppm). This information is further explained in Table 1, which summarizes the treatments and experimental groups.

Table 1 A summary of the treatments and experimental groups.

Treatment Group	P Concentration	Dust Application Method	CO2 Condition	Replicates (n)
-P treatment (P-deficient)	0.1 mg/L	Foliar (Desert Dust)	412 ppm	6
-P treatment (P-deficient)	0.1 mg/L	Foliar (Volcanic Ash)	412 ppm	6
-P treatment (P-deficient)	0.1 mg/L	Root (Desert Dust)	412 ppm	6
-P treatment (P-deficient)	0.1 mg/L	Root (Volcanic Ash)	412 ppm	6
+P treatment (P-sufficient)	Full P	No Dust	412 ppm	6
-P control (untreated)	0.1 mg/L	No Dust	412 ppm	6
-P treatment (P-deficient)	0.1 mg/L	Foliar (Desert Dust)	850 ppm	6
-P treatment (P-deficient)	0.1 mg/L	Foliar (Volcanic Ash)	850 ppm	6
-P treatment (P-deficient)	0.1 mg/L	Root (Desert Dust)	850 ppm	6
-P treatment (P-deficient)	0.1 mg/L	Root (Volcanic Ash)	850 ppm	6
+P treatment (P-sufficient)	Full P	No Dust	850 ppm	6
-P control (untreated)	0.1 mg/L	No Dust	850 ppm	6

Table 1 Experimental design summarizing treatments, P concentrations, dust application, CO_2 conditions, and replicates.

To mimic dust deposition which typically occurs during a few major desert storms or volcanic eruptions each year, we applied the dust in two equivalent doses between 35-42 days after germination. We calculated the average foliar area of the chickpea pots, taking into consideration the planting density, and correcting values for the area covered by an individual plants. These values were used to determine the total application mass. In total, the average application mass was 3 g per pot, simulating the total dust deposition per square meter over the growing season in southern Israel. This method was based on our previous studies (Gross et al, 2021, Starr et al, 2023,

163   Lokshin et al, 2024). The dust treatments were done either directly on the foliage while covering the pot,

164   preventing the dust from touching the roots, or directly on the roots where the pots were subsequently covered

165   with nylon to equalize conditions with the foliage treated plants. Afterwards, the plants were left undisturbed with

166   the settled dust particles on their foliage or surface of the root area.

167   Among the control plants, 12 plants received the +P fertigation and 12 additional plants received -P fertigation.

168   Each treatment group was divided into two CO_2 levels, 36 plants in each CO_2 growing room. The plants were

169   harvested 10 days after the last dust application (55 days after germination). To ensure that nutrients from dust

170   particles were not washed by the irrigation during the experiment, we monitored the total P (i.e., P that dissolves

171   in strong acid) in the water that drained from the pots (Longo et al., 2014; Gross et al., 2015) throughout the

172   experiment.

173   We performed a parallel experiment under aCO_2 where we grew six additional plants, in larger 5 L pots, filled

174   with soil, to test whether our findings also apply to natural soil conditions (Fig. S1).

2.2 Mineral dust material

176   We applied plant foliage and the area near plants' roots, with desert dust and volcanic ash, the two main mineral

177   dust types in the atmosphere (Langmann, 2013b). To achieve enough mass for our experiment, we produced dust

178   analogs from surface desert soil and surface volcanic ash soil, following procedures described by others (Gross et

179   al., 2021; Stockdale et al., 2016). The desert dust analog surface soil was collected from the southern Israel Negev

180   desert (30°320N 34°550E) (Gross et al., 2021). Chemical and mineralogical properties of the resulted dust are

181   comparable to dust collected in the Sahara and other places in the Middle East (Gross et al., 2016a; Palchan et al.,

182   2018). The volcanic ash analog was collected from Mount Etna (Sicily, Italy) two months after the eruption of 21

183   February 2022. The ash was taken from the upper cable car station "Funivia dell'Etna" (37°704N, 14°999E). The

184   samples were then processed through a setup of sieves to achieve a particle size smaller than $63\mu m$ that are

185   considered windblown (Guieu et al., 2010). The chemical and mineralogical properties of the dust analogs are

186   presented in Table 2.

2.3 Plant biomass and elemental analysis

189   After harvesting, the plants were separated for roots and shoots, washed in 0.1M HCl and rinsed three times in

190   distilled water to remove dust particle residue (Gross et al., 2021; Lokshin et al., 2024a). To ensure that the

191   washing procedure removed all the applied dust particles from the leaf surfaces, we scanned surfaces of randomly

192   selected dusted and washed leaves with SEM-EDS which combines scanning electron microscope and energy-

193   dispersive X-ray spectroscopy to detect and analyze materials. After washing, plant tissue was dried, weighed and

194   root and shoot biomass were recorded. Afterwards, the dry shoot material was ground to powder and dry ashed at

195   550 C° in a furnace for four hours (Tiwari et al., 2022). Approximately 1g of the ashed material was subsequently

196   dissolved using 1 mL concentrated HNO_3 to achieve a clear solution. To prepare the dust types for elemental

197   analysis, the samples were dissolved on a hotplate by sequential dissolution using concentrated HNO_3, HF, and

198   HCl, resulting in clear solutions (Palchan et al., 2018). The elemental composition of the plants, dusts and nutrient

199   solution were analyzed at the Hebrew University using ICP-MS (Agilent 8900cx; Agilent Technology). Prior to

200   analysis, the ICP-MS was calibrated with a series of multi-element standard solutions (1 pg/mL - 100 ng/mL

201   Merck ME VI) and standards of major metals (300 ng/ml - 3 mg/mL). Internal standard (50 ng/mL Sc and 5 ng/mL

202   Re and Rh) was added to every standard and sample for drift correction. Standard reference solutions (USGS SRS

203   T-207, T-209) were examined at the beginning and end of the calibration to determine accuracy. The calculated

204   accuracies for the major and trace elements are 3% and 2%, respectively.

205   **2.4 Leaf surface pH**

206   Leaf surface pH was measured by manually attaching a portable pH electrode designed for flat surfaces (HI-1413;

207   HANNA pH instruments) onto the surface of three leaves from each plant. The measurements were performed

208   four times throughout the growing season (19, 24, 35 and 40 DAG) in the morning, two hours after sunrise.

209

210   **2.5 Trichome density**

211   Trichome density was determined in four young, fully developed leaves from four different plants per variety in

212   the P- treatment only (n=16). Leaves were scanned in a scanning electron microscope (VEGA3; Tescan, Czech

213   Republic). From each leaf, three photos of a $1mm^2$ field were taken, and glandular and regular trichomes were

214   counted.

215

216   **2.6 Leaf exudates**

217   For analysis of the organic exudates, 2g of fresh leaves were sampled randomly from the P+ and P- treatments

218   before harvesting. The leaves were rinsed in 2 ml of distilled water and methanol (50:50) for 10 s. The extracted

219   surface metabolites were supplied with 50 µL of internal standard (ribitol, 0.2 mg ml^{-1}) and stored at -80°C until

220   analysis. Before analysis, the extracted samples were vacuum dried overnight at 35°C. The dried material was

221   redissolved in 40 µl of 20 mg mL^{-1} methoxamine hydrochloride (CH_3ONH_2 HCl) in pyridine (C_5H_5N) and

222   derivatized for 90 min at 37°C, followed by a spike of 70 µL MSTFA (*N*-methyl-*N* (trimethylsilyl)

223   trifluoroacetamide ($CF_3CON(CH_3)Si(CH_3)_3$) at 37°C for 30 min**.** The dissolved metabolites were then introduced

224   to a mass spectrometry gas chromatograph (Agilent 6850 GC/5795C; Agilent Technology) for analysis. The

225   metabolites were detected by a mass spectrometer, where 1 µL of each sample was injected in split-less mode at

226   230°C to a helium carrier gas at a flow rate of 0.6 mL min^{-1}. GC processing was carried out using an HP-5MS

227   capillary column (30 m 9 0.250 mm 9 0.25 µm) and the spectrum was scanned for *m/z* 50–550 at 2.4 Hz. The ion

228   chromatograms and mass spectra obtained were evaluated using the MSD CHEMSTATION (E.02.00.493)

229   software, and sugars and amino acids were identified via comparison of retention times and mass spectra with

230   certified GC plant metabolite standards (Sigma Aldrich).

231

232   **2.7 Nd isotopes**

233   We characterized the radiogenic Nd isotope compositions of desert dust, volcanic ash, and the different treated

234   and control plants to evaluate the ion flux from the foliage into the plant. The use of Nd isotopes is common in

fingerprinting studies in various fields (Aciego et al., 2017; Arvin et al., 2017; Chadwick et al., 1999) as it is a refractory element that has virtually no fractionation and reflects the composition of its source. In our experiments the control plants reflect the original composition of the plant and deviation from it can only occur if ions were supplemented through nutrient uptake. Nd was extracted by ion chromatography using specialized resins, first TRU resin to separate the REEs followed by LN-spec to separate Nd from Sm (following Palchan et al., 2013). The isotope ratios were measured using a Thermo Neptune multi-collector ICP-mass spectrometer at the Weizmann Institute of Science. Along with the samples we measured several standards to ensure quality and accuracy of the measurements. Standard JNdi bracketed every five samples, resulting with $^{143}Nd/^{144}Nd$ value of 0.512035 ± 10 (2σ, n=60). We normalized the data to $^{143}Nd/^{144}Nd = 0.512115$ (Tanaka et al., 2000). Standard BCR-2 was dissolved and analyzed along with the plant and dust samples yielding $^{143}Nd/^{144}Nd$ value of 0.512628 ± 6 (2σ, n=3) that agrees with $^{143}Nd/^{144}Nd = 0.512637 \pm 13$ (Jweda et al., 2016) . We present the Nd isotope ratios in the epsilon notation:

$$\varepsilon_{Nd} = \left(\frac{\left(\frac{^{143}\text{Nd}}{^{144}\text{Nd}} \right)_{\text{Sample}}}{\left(\frac{^{143}\text{Nd}}{^{144}\text{Nd}} \right)_{\text{CHUR}}} - 1 \right) \times 10,000$$

where the value of $^{143}Nd/^{144}Nd = 0.512638$ in CHUR (Wasserburg et al., 1981). A sample isotopic characterization is given in Table S1. We calculated the % of foliar contribution using simple mixing equation of two components:

$$\% \, Foliar \, contribution = \frac{\varepsilon Nd_{sample} - \varepsilon Nd_{control}}{\varepsilon Nd_{end \, member} - \varepsilon Nd_{control}} * 100$$

where εNd_{sample} refers to plants that were treated either with desert dust or volcanic ash with, $\varepsilon Nd_{control}$ refers to the untreated control plants and $\varepsilon Nd_{endmember}$ are the measured end member values of -10.3 for desert dust or 4.5 value for volcanic ash (Table S1 & Fig. 4). The calculation was done separately on the two different treatments (i.e., desert dust and volcanic ash).

2.8 Mineralogical analysis

 Mineralogical composition of the dusts was determined with an X-ray powder diffraction (XRD) using a Panalytical Empyrean Powder Diffractometer equipped with a position sensitive X'Celerator detector. Cu Kα radiation (k = 1.54178_A) at 40 kV and 30 mA. Scans were done over a 2h period, between 5° and 65° with an approximate step size of 0.033°.

2.9 Statistical Analysis

Treatment comparisons for all measured parameters were tested using post-hoc Tukey honest significant difference (HSD) tests ($P < 0.05$). The significant differences are denoted using different letters in the figures.

`

 The standard errors of the mean in the vertical bars (in the figures) were calculated using GraphPad Prism version
273 9.0.0.

274

275 **3 Results**

276 **3.1 Plant biomass and total P under aCO$_2$ and eCO$_2$**

277 Shoot biomass of the +P plants are significantly larger than -P plants. Among +P plants, those grown under
278 elevated eCO$_2$ conditions are significantly larger than those grown under ambient aCO$_2$ conditions ($p < 0.001$,
279 table 2). In contrast, -P plants grown under eCO$_2$ exhibit similar biomass to -P plants grown under aCO$_2$ ($p =$
280 0.99, table 2). The impact of foliar desert and volcanic dust application was reflected by the increase of their
281 biomass and total P content through shoot biomass gain rather than through changes in shoot P concentration. As
282 such, the P contribution in the dusted plants was expressed in increased aboveground plant biomass rather than in
283 increased P concentrations in tissues (Table 2), probably as plants distributed the extra P to support growing
284 biomass. Thus, the treatment effects are reflected by changes in total plant P (concentration multiplied by shoot
285 biomass). Under aCO$_2$ conditions, desert dust application resulted in shoot biomass and total P content increases
286 of 35% and 21%, respectively, and volcanic ash application resulted in 28% and 35% increases, respectively (Fig.
287 1 d,f). The root-treated plants did not show any increases in the shoot biomass or total P content (Fig. 1 c,e). These
288 trends are also seen in the eCO$_2$ conditions of 850 ppm atmospheric CO$_2$ experiment. Desert dust application
289 resulted in shoot biomass and total P content increases of 29% and 20%, respectively, and volcanic ash application
290 resulted in 62% and 51% shoot biomass increases, respectively (Fig. 2 d, f). Similarly, the root-treated plants did
291 not show any increases in the shoot biomass or total P content (Fig. 2 c, e). Unlike the shoots, no significant
292 changes of the biomass of the roots were detected across all treatments, thus changes in the root shoot ratio reflect
293 variations in shoot biomass rather than root biomass (Table 2).

294

295

296

297

298

299
300
301
302
303

304 **Table 2** Shoot and root biomass, root-to-shoot ratio, phosphorus (P) concentration, and total P content in *Cicer arietinum* cv.
305 'Zehavit' under different treatments.

306

307

Plant material	Shoot biomass (g)	p_value shoot biomass	Root biomass (g)	p_value root biomass	Root/Shoot ratio	p_value root/shoot ratio	P (µg/g)	p_value P	Total P (P*shoot biomass)	p_value total P
Control '-P' 412 ppm CO_2 **average** value	1.36		1.17		0.86		726		984	
Control '-P' 412 ppm CO_2 **standard** deviation	0.22		0.22		0.07		78		162	
Control '-P' 850 CO_2 ppm **average** value	1.50		1.22		0.82		712		1050	
Control '-P' 850 CO_2 ppm **standard** deviation	0.25		0.20		0.05		89		77	
'-P' + foliar application of desert dust 412 ppm CO_2 - **average** value	1.95	0.004*	1.57	0.05	0.81	0.04	833	0.723	1664	0.141
'-P' + foliar application of desert dust 412 ppm CO_2 - **standard** deviation	0.24		0.21		0.08		366		917	
'-P' + foliar application of desert dust 850 ppm CO_2 - **average** value	1.93	0.013*	1.55	0.271	0.81	0.10	663	0.753	1258	0.026
'-P' + foliar application of desert dust 850 ppm CO_2 - **standard** deviation	0.24		0.26		0.16		125		151	
'-P' + foliar application of volcanic ash 412 ppm CO_2 - **average** value	1.84	0.0055*	1.39	0.31	0.75	0.99	769	0.946	1416	0.006*
'-P' + foliar application of volcanic ash 412 ppm CO_2 - **standard** deviation	0.27		0.27		0.04*		57		207	
'-P' + foliar application of volcanic ash 850 ppm CO_2 - **average** value	2.42	0.001*	2.05	0.004*	0.84	0.94	674	0.846	1607	<0.0001*
'-P' + foliar application of volcanic ash 850 ppm CO_2 - **standard** deviation	0.39		0.44		0.07		105		168	
Control '+P' 412 ppm CO_2 **average** value	10.74	<0.0001*	4.01	<0.0001*	0.37	<0.0001*	2123	<0.0001	22796	<0.0001
Control '+P' 412 ppm CO_2 **standard** deviation	0.71		0.66		0.04		225		2654	
Control '+P' 850 ppm CO_2 **average** value	15.99	<0.0001*	7.98	0.0015*	0.50	0.02	2417	0.143	38593	0.001*
Control '+P' 850 ppm CO_2 **standard** deviation	1.86		1.94		0.10		363		6875	

Fertilizers and dusts (ppm)	Mg (mg/g)	P (µg/g)	K (mg/g)	Ca (mg/g)	Mn (mg/g)	Fe (µg/g)	Ni (µg/g)	Cu (µg/g)	Zn (µg/g)
+P fertilizer	1.26	713	6.00	0.01	0.1	0.15	0.4	5.6	50.1
-P fertilizer	1.21	35	7.80	0.01	0.1	0.13	0.4	5.1	47.5
Desert dust	6.50	1387	8.60	136	0.24	12.7	18.0	10.0	39.0
Volcanic ash #1	23.5	1669	12.5	64.4	1.1	63.7	49.5	118.6	80.0
Volcanic ash #2	22.6	1788	12.0	61.6	1.1	61.9	48.3	115.6	73.7

Table 2 The p-values indicate statistical comparisons for each parameter: (i) dust and ash applications under aCO₂ compared to the aCO₂ control, (ii) dust and ash applications under eCO₂ compared to the eCO₂ control, (iii) +P plants under aCO₂ compared to -P plants under aCO₂, and (iv) +P plants under eCO₂ compared to +P plants under aCO₂. The final section presents the elemental composition of the dust, ash, and fertilizers used in the experiment (ICP-MS analysis). Nutrient concentrations are expressed in µg/g for micronutrients and mg/g for macronutrients.

Root treatment 412 ppm   **Foliar treatment 412 ppm**

a b

c   d

e f
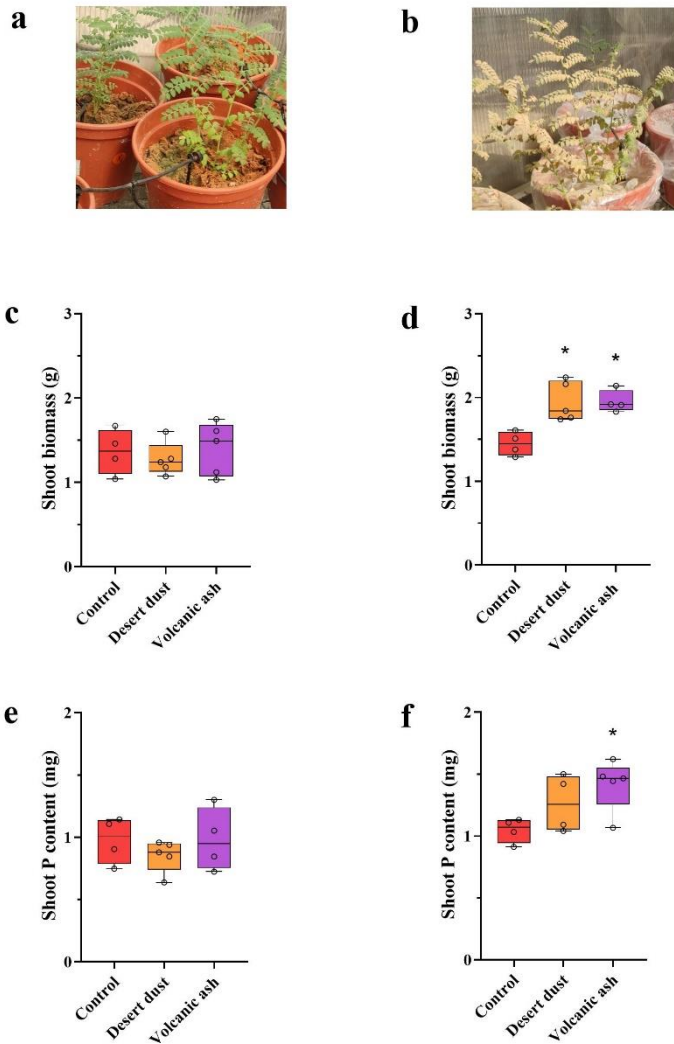
Figure 1 (a-f): Biomass and total P content increases due to dust application treatments at aCO₂ of 412ppm. (a) Image of experiment setting of the root treatment. *Image was taken immediately after the dust application. (The actual amount of dust remaining on the plant leaves at the end of the experiment was significantly smaller than what is depicted in the picture image).* (b) Image of experiment setting of foliar treatment. (c) Shoot biomass of root treated plants. (d) Shoot biomass of foliar treated plants. (e) Shoot total P content of root treated plants. (f) Shoot total P content of foliar treated plants. The red color represents control plants, orange desert dust treatment and purple volcanic ash treatment. Asterisks represent statistically significant differences in response to foliar application of desert dust and volcanic ash ($P < 0.05$, one-way ANOVA with Tukey's post hoc test). The box and whiskers plots represent the distribution of the data. The central line indicates the median, the edges of the box correspond to the 25th (Q1) and 75th (Q3) percentiles, and the whiskers span from the minimum to the maximum values. Individual data points (n = 5) are overlaid on the plot to illustrate the full distribution.

345

Root treatment 850 ppm   Foliar treatment 850 ppm
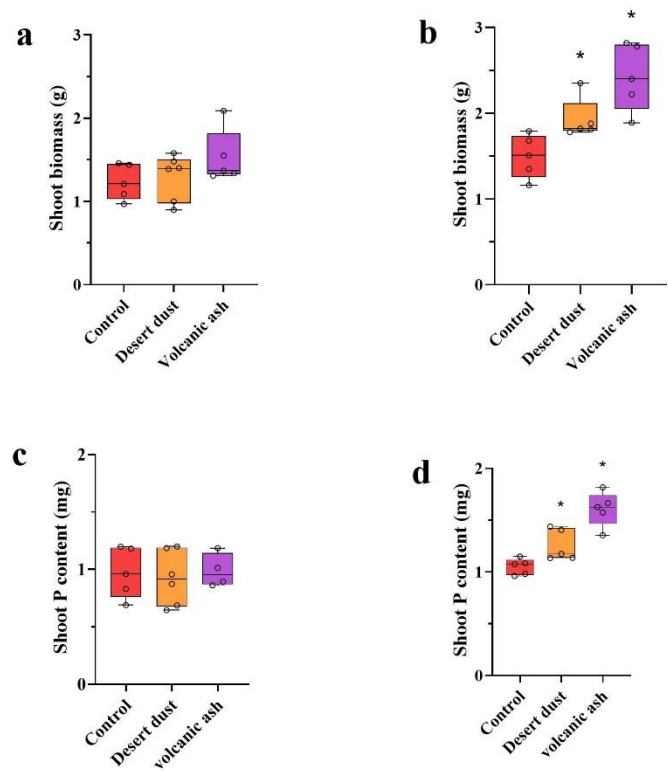
360

Figure 2 (a-d): Biomass and total P content increases due to dust application treatments at eCO$_2$ of 850ppm. (a) Shoot biomass of root treated plants. (b) shoot biomass of foliar treated plants. (c) Shoot total P content of root treated plants. (d) Shoot P content of foliar treated plants. The biomass and total P content in the root treated plants do not show increases compared with the control groups. The red color represents control plants, orange desert dust treatment and purple volcanic ash treatment. Asterisks represent statistically significant differences in response to foliar application of desert dust and volcanic ash (P < 0.05, one-way ANOVA with Tukey's post hoc test). The box and whiskers plots represent the distribution of the data. The central line indicates the median, the edges of the box correspond to the 25th (Q1) and 75th (Q3) percentiles, and the whiskers span from the minimum to the maximum values. Individual data points (n = 5) are overlaid on the plot to illustrate the full distribution.

370

371

372

373

`

374 **3.2 Biochemical properties of chickpea varieties**

375 The domesticated variety 'Zehavit' showed a strong response to the foliar treatment with up 35% increased

376 biomass compared to the control group, whereas the wild variety CR934 showed up to 5% increases compared

377 with the control group (Fig. 3a). The leaf pH of the Zehavit was 1.15 and of the CR934 it was 2.7 (Fig. 3b),

378 trichome density, both glandular and non-glandular, were higher in the Zehavit compared to the CR934 (Fig. 3c-

379 e). The exudates of oxalic, malic, and citric acids were significantly higher at the Zehavit in comparison to CR934

380 (Fig. 3f). The results indicate increased biomass, lower pH, higher trichome density, and higher exudate levels in

381 the 'Zehavit' variety.

382 **3.3 Shoot nutrient status under eCO_2 conditions**

383 To quantify the impact of elevated eCO_2 conditions on the nutrient status of plant samples, we conducted a

384 comparison between the ionome of chickpea plants grown under aCO_2 and those grown under eCO_2 levels for

385 both foliar fire ash treated and untreated plants. The comparison was conducted as follows: the average value of

386 each nutrient in plants grown under aCO_2 was calculated, and then each nutrient in individual chickpea plants

387 grown under eCO_2 levels was expressed as a ratio relative to the average under aCO_2 conditions (eCO_2 plant (each

388 individual plant) / aCO_2 plant (average of all the control plants). We observed that eCO_2 conditions led to a reduction in the

389 concentrations of Mg, K, Ca, Mn, Zn, Cu, Fe, and Ni, ranging from 29% (Fe) to 90% (Ni). The foliar desert dust and volcanic

390 ash treated plants indicate a significant increase in the concentration of Fe and Ni (Fig. 5).

391

`
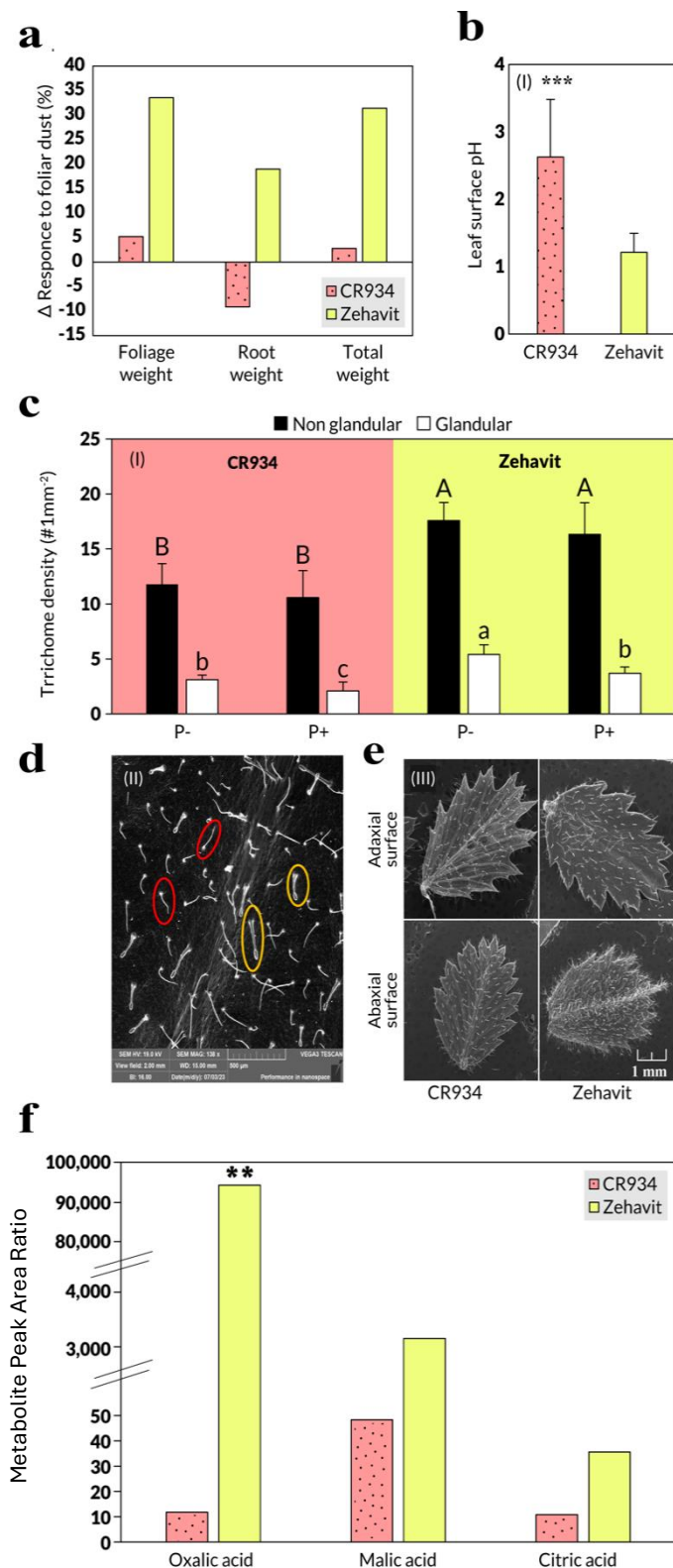
Figure 3 (a-f): Comparison of two chickpea varieties - CR934 (dotted, pink) and Zehavit (yellow) and their leaf properties under dust foliar fertilization. (a) Biomass and P uptake response to foliar dust P. Each column indicates the difference Δ (%) between the foliar dusted plants and the control untreated plants (n=6). (b) (I) Leaf surface pH. Each value indicates an average of five measurements on a plant throughout the growth season in control treatment (n=90), and two measurements in foliar dust treatment (n=10). Three asterisks indicate significant differences between treatments using a T-test, and a one-way ANOVA (P≤0.001). (c) Leaf non-Glandular (black column) and glandular (white column) trichrome density in CR934 and Zehavit control plants (-P and +P). Different letters indicate significant differences between varieties and treatments using Tukey-HSD test (P≤0.05) (n=12). Capital letters refer to non-glandular trichomes and small letters refer to glandular trichomes. (d). SEM scans of non-glandular (red circles) and glandular (yellow circles) trichomes of typical Zehavit leaf. (e). SEM scans of leaves of CR934 (left) and Zehavit (right) varieties.. (f). Exudates of organic acids. Each column indicates the average of leaf washing from four plants, in P- control treatment (n=4). Values are normalized to an internal standard (ribitol) for comparability. Two asterisks indicate significant differences between treatments using a T-test, and a one-way ANOVA (P≤0.01). Values are concentrations compared with an internal standard.

409

410
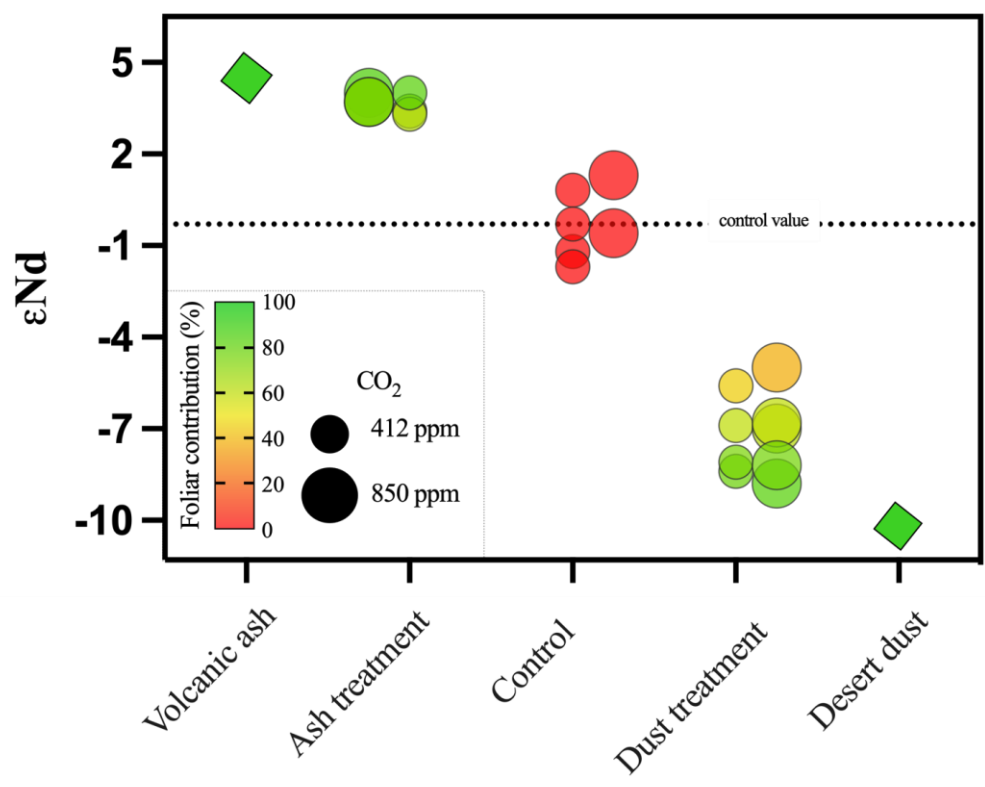
Figure 4: Quantification of dust mineral-nutrient flux from foliage. Radiogenic isotopic ratios of $^{143}Nd/^{144}Nd$ in the different sample groups (x-axis) expressed in εNd values. Diamonds represent the two applied mineral fractions of volcanic ash and desert dust; circles represent plants treated with the desert and volcanic dusts and the control groups. Large circles represent plants growing in the 850 ppm eCO_2 and small circles represent the 412 ppm aCO_2. The color scale reflects the % contribution of Nd originating from the dusts via the foliage, which was calculated using a two-component mixing model. The control plants' Nd signature reflects the inheritance value from the seed, where a value of εNd=-0.3 is set as the control, εNd=-10.3 as the desert dust value, and εNd=4.6 as the volcanic ash value. A foliar contribution of more than 60% is evident in the plants applied with desert dust and more than 70% in the plants applied with volcanic ash. Standard errors on the isotopic values are all smaller than the depicted data points.

411
412
413
414
415
416
417
418
419
420
421
422
423
424
425
426
427
428
429

a

444

b
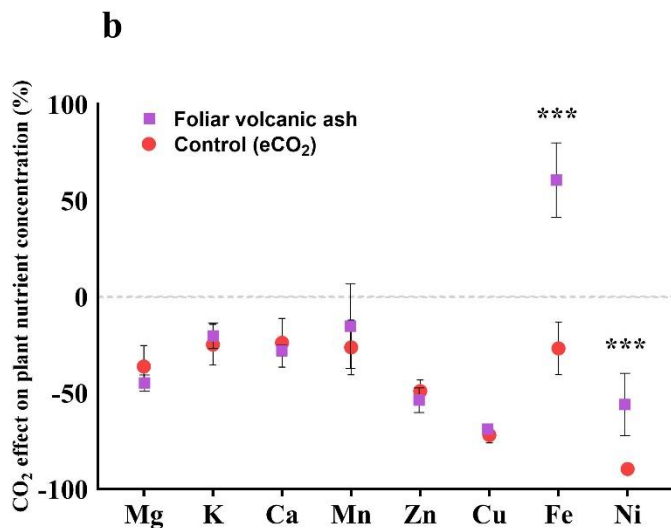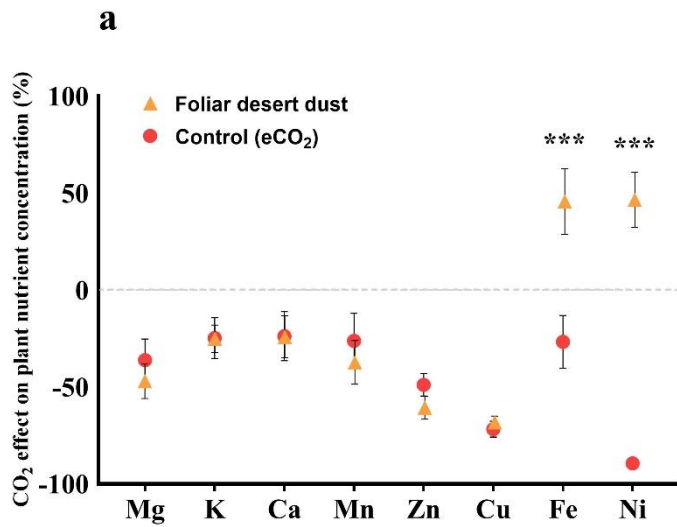
Figure 5 (a-b) Comparison of the % change in plant nutrient concentration under eCO_2 compared with aCO_2 control plants. The dashed line represents the average values of the control plants grown under aCO_2 levels; the values below the dashed line indicate a decline in the respective nutrient under eCO_2 levels. (a) The effect of foliar treatment of desert dust (orange triangles). (b) The effect of foliar treatment of volcanic ash (purple squares). Asterisks indicate statistically significant differences in response to foliar application of desert dust and volcanic ash ($P < 0.05$, one-way ANOVA with Tukey's post hoc test). Error bars represent standard deviations (n = 5).

469

470

471

472

473 **4 Discussion**

474

475 **4.1 Foliar mineral-nutrients uptake**

476 In our experiments, we simulated desert dust and volcanic ash deposition by manually applying them on chickpea

477 plants (*Cicer arietinum cv 'Zehavit'*). The dust was applied separately either on the surface of the pot near the

478 roots, or on its foliage (Fig. 1), while control plants were not treated with dust. After several weeks, a significant

479 impact of the foliar treatment was already noticeable where shoot biomass and total P content in the foliage-treated

480 plants had increased, following dusts treatment, compared with the control group. In contrast, the root-treated

481 plants did not show any increases in the biomass or P content, suggesting that over short timescales (i.e., several

482 weeks), foliar uptake is the only nutrient uptake pathway from freshly deposited dust (Fig. 1c, e). These results

483 were then replicated when a similar experiment was conducted with plants grown on sandy soil, in bigger pots

484 (Fig. S1), emphasizing that our observations are not limited to the specific artificial experimental conditions in

485 perlite (which may bias root behavior), but also apply for real soil conditions (Fig. S1).

486 **4.2 Foliar mineral-nutrient uptake mechanisms**

487 Most of the P in dust is incorporated in the mineral lattice of minerals such as apatite (Dam et al., 2021), which is

488 largely insoluble under the natural rhizosphere pH range (Hinsinger, 2001). Hence, P in volcanic or desert dust

489 has low bioavailability for root uptake as was also shown in Lokshin et al, (2024a) with fire ash. On the leaf

490 surface however, chemical, morphological, and microbial modifications may promote nutrient solubility and

491 bioavailability and thus enable uptake through the leaf surface (Gross et al., 2021; Muhammad et al., 2019).

492 Examining two chickpea varieties with contrasting responses to dust application: wild variety CR934, and

493 common domesticated variety Zehavit, we found a few properties that facilitate foliar P acquisition from dust

494 (Fig. 3). These include structural, morphological, and chemical modifications that are comparable to those

495 reported in the rhizosphere (Hinsinger, 2001). The foliar-uptake-efficient variety Zehavit has significantly more

496 acidic leaf surface (pH ~ 1, Fig. 3b), and thus promotes both dissolution and mobility of P from the pH sensitive

497 mineral apatite (Gross et al., 2015), as well as other mineral-nutrients in the dust (Bradl, 2004; Gross et al., 2021;

498 Muhammad et al., 2019). Nutrient uptake through the leaf is mediated by two primary pathways: the cuticle and

499 stomata (Eichert and Fernández, 2022). The cuticle, while a hydrophobic barrier, contains dynamic aqueous

500 pathways that allow solutes to diffuse, particularly under high humidity. Stomata act as regulated pores,

501 facilitating the direct uptake of hydrophilic solutes and dissolved nutrients. These mechanisms likely complement

502 the observed properties in Zehavit, where acidic exudates such as oxalate and malate further facilitated P uptake

503 by promoting the dissolution of insoluble P forms (Lambers et al., 2019; Tiwari et al., 2022). Similarly, increased

504 sugar levels, such as glucose and sucrose (Fig. 3f, fig. S2), likely stimulated the activity of nutrient-solubilizing

505 microbes on the phyllosphere (Shakir et al., 2021). Additionally, Zehavit displayed higher trichome density on

506 both leaf axial and adaxial surfaces (Fig. 3 c,d,e). These trichomes not only enhance metabolite release but also

507 improve dust adhesion, increasing the contact time for nutrient solubilization and uptake (Gross et al., 2021) (fig.

`

508 S3). Together, these traits align with established foliar uptake pathways and highlight the synergistic roles of
509 chemical, morphological, and microbial modifications in facilitating nutrient acquisition from dust."

510 . We postulate that other plant species share comparable leaf traits that enhance dust capture and solubility such
511 as wheat and various tree species that showed strong responses to foliar dust fertilization (Gross et al., 2021; Starr
512 et al., 2023). Overall, our results suggest that the combination of leaf surface acidification, secretion of organic
513 acids and additional exudations combined with an increased trichome density enhances foliar dust capture and
514 nutrient uptake in chickpeas.

515

516 4.3 Dust Shading, Photosynthesis, and Elevated CO_2 Effects

517 Desert dust deposition on plant foliage exhibits both beneficial and harmful effects, influenced by its physical and
518 chemical attributes as well as environmental conditions. Starr et al. (2023) demonstrated that dust application can
519 impact trees both positively and negatively: while it increased phosphorus (P) concentrations in some species,
520 total plant P content showed only mild or stagnant increases, suggesting limited P utilization due to antagonistic
521 dust–leaf interactions. On the harmful side, dust reduced final biomass across tree species, likely through
522 disruptions in photosynthesis, stomatal conductance, and other physiological processes. Species-specific
523 responses were noted, such as significant reductions in carbon assimilation and biomass in Schinus and a notable
524 58% biomass reduction in Quercus. Similarly, Lokshin et al. (2024b) observed an initial reduction in carbon
525 assimilation following dust application, likely due to shading effects or stomatal occlusion. However, the
526 increased content of rare earth elements (REE) resulting from foliar dust application subsequently contributed to
527 improving carbon assimilation. In contrast, Gross et al. (2021) found no significant impact on plant biomass when
528 using inert silica dust, suggesting that the effects of dust strongly depend on its chemical composition. They also
529 proposed that negative impacts might be mitigated by plants increased internal P demand.

530 4.4 Dust impact on plant nutrient status under eCO_2

531 Numerous studies reported that eCO_2 conditions reduce the concentrations of several nutrients in plant tissues
532 such as Fe, Zn, Cu, Mn, Ni and others (Loladze, 2002; Fernando et al., 2014; Myers *et al.*, 2014; Gojon *et al.,*
533 2023). The reduction in shoot nutrient concentrations was also observed in our experiments (fig. 5). In accordance
534 with previous knowledge (Loladze, 2002), plants that were grown under eCO_2 in our experiment showed a
535 significant reduction in the concentrations of nutrients (Fig. 5). Although we did not observe statistically
536 significant differences in biomass between control plants grown under aCO_2 and eCO_2 conditions (P = 0.4), the
537 reduction in essential macro- and micronutrient concentrations may be partly explained by the effect of nutrient
538 dilution. Another potential reason for the nutrient decline under eCO_2 could be related to reduced efficiency in
539 mineral nutrient absorption through the root system (Gojon et al., 2023). We found that foliar application of both
540 volcanic and desert dust on plants that were grown under eCO_2 replenished their Fe and Ni concentrations (both
541 essential micronutrients for plant growth and in the human diet) compared with the control group (fig, 5a,b).
542 Desert dust treated plants showed increases of Fe and Ni concentrations of 44% and 46%, respectively (Fig. 5a).
543 Volcanic ash treated plants showed Fe elevated concentrations of 66% (Fig. 5b). The Ni concentrations had more
544 moderate increases from volcanic ash, with 40% higher than in the aCO_2. These increases returned Fe and Ni back

545   to standard, nontoxic levels (Shahzad et al. 2018). These results suggest that the role of foliar uptake of

546   atmospheric nutrients in the mineral nutrition level of plants may increase under eCO_2, potentially offsetting some

547   of the nutrient reduction driven by the dilution effect and the downregulation of the root nutrient uptake pathway

548   (Zhu et al., 2018). Despite adhering strictly to the washing protocol described in Gross et al. (2021) and Lokshin

549   et al. (2024a), we acknowledge that some dust particles may remain on the plant surfaces. However, their influence

550   on the results is negligible, as the contribution of any residual particles to the measured values is minimal and

551   does not affect the overall interpretation of the results.

552

553   **4.5 Quantifying the contribution of foliar nutrient uptake from dust**

554   Traditionally, radiogenic Nd isotopes serve as excellent tracers for sources of magmatic rocks (Stein and

555   Goldstein, 1996), sediment archives (Chadwick et al., 1999; Palchan et al., 2018), and water bodies (Farmer et

556   al., 2019). Since Nd is found in high concentration in nutrient bearing minerals (Aciego et al., 2017; Arvin et al.,

557   2017; Chadwick et al., 1999), Nd isotopes were recently used to trace P sources in plant tissues, where it was

558   shown that the contribution of dust outpaces the weathering of the local bedrock over geological time scales

559   (Aciego et al., 2017; Arvin et al., 2017). While the use of Nd isotopes to other elements such as P provides new

560   knowledge on their sources, it should be done cautiously because different elements have differing speciation,

561   uptake mechanisms, and transport kinetics in plant tissue. Here, we utilized the ratio of $^{143}Nd/^{144}Nd$ in the εNd

562   notation to trace the source of Nd in our experiments and quantify its flux to plant tissue from dust. From this

563   measurement we can approximate the flux of P, Fe and Ni via foliar pathway (Fig. 4). We used a two-component

564   mixing model, where the average εNd value of the control plants, -0.3, which arise from the Nd "inheritance"

565   (i.e., the Nd composition of the seed, since the amount of Nd in the chemical fertilizer was negligible) is regarded

566   as one end member, and dust εNd values are regarded as the second end member, with values of -11 (desert dust)

567   and 5 (volcanic ash). We found that desert dust treated plants were characterized with εNd values of -8.8 to -5,

568   significantly different than the inheritance value of the control group. Similarly, the volcanic ash treated plants

569   were characterized with εNd values of 3.4 to 4, significantly different than the inheritance value of -0.3. Thus, it

570   is evident that the εNd of the foliage-treated plants comprise a mixture of the inheritance and the type of dust

571   applied. Based on the mixing model, the chickpea plant acquired over 60% of its Nd from desert dust deposited

572   on the foliage. Volcanic ash deposited on the foliage contributed over 70% of its Nd (Fig. 4). However, Nd

573   isotopes do not show the increased supplement of Fe and Ni in plants that were grown under eCO_2. Thus, more

574   data on the relation between Nd and other nutrients uptake will advance its use in future studies to quantify the

575   immediate contribution of freshly deposited dust on plants nutrition in field and lab experimental settings.

576

577   In conclusion, we showed here that dust nutrient uptake via the foliar pathway in responsive chickpea plants play

578   a significant role in their nutrition under P limited conditions. Plant foliage captures and dissolves freshly

579   deposited dust particles, making atmospheric mineral nutrients more accessible through the foliage on a short time

580   scale than via the roots. Most of the P in the dust is incorporated in the mineral lattice of minerals such as apatite

581   (Dam et al., 2021), which is largely insoluble under the natural rhizosphere pH range (Hinsinger, 2001). Hence,

582   P in dust has low bioavailability for root uptake. On the leaf surface however, chemical, morphological, and

583   microbial modifications may promote nutrient solubility and bioavailability and facilitate uptake through the leaf

`

surface (Gross et al., 2021; Muhammad et al., 2019). Thus, our findings highlight that dust serves as an alternative source of nutrients to plants from the foliage on short timescales of a few weeks. Furthermore, foliar dust acquisition compensates for the reduction in nutrients such as Fe and Ni, induced by eCO_2 conditions (Gojon et al., 2023). The broader aspect of our findings emphasizes the central role of dust in plant nutrition through the foliar pathway and to global biogeochemical cycles. Our findings suggest that foliar uptake from natural dust could be a relevant pathway under future elevated CO_2 conditions, and that this pathway may be a target for novel fertilization techniques to compensate for the expected decline in the crops' nutritional value.

Acknowledgments:

We thank Dr. Yigal Erel and Ofir Tirosh from the Hebrew University of Jerusalem for their support in ICP-MS analyses, and Dr. Yael Kiro from Weismann Institute for conducting isotopic chromatography in her lab, and Dr. Sthephen Fox for his support in MC-ICP-MS analyses.

Financial support:

This research has been supported by the Keren Kayemeth LeIsrael-Jewish National Fund (KKL-JNF) climate team doctoral fellowship and the Israeli Science Foundation (ISF) (grant no. 144/19 and grant no. 267/24). In addition, this research was partly supported by Research Grant Award No. IS-5443-21 R, from BARD, The United States - Israel Binational Agricultural Research and Development fund.

Author Contributions:

Conceptualization: DP, AG, RE

Dust sampling: AL, DA, AG

Methodology: DP, AG, RE

Investigation: AL, EG, SF

Visualization: DP, AL, EG

Funding acquisition: AG, RE, AL

Project administration: DP, AG

Supervision: DP, AG, RE

Writing – original draft: DP, AG, AL, RE

Competing Interest Statement: The authors declare no competing interests.

Classification: Physical Sciences - Earth, Atmospheric, and Planetary Sciences; Biological Sciences - Plant Biology.

`

616 **References**

617 Aciego, S. M., Riebe, C. S., Hart, S. C., Blakowski, M. A., Carey, C. J., Aarons, S. M., Dove, N. C., Botthoff, J.
618 K., Sims, K. W. W., and Aronson, E. L.: Dust outpaces bedrock in nutrient supply to montane forest ecosystems,
619 Nat Commun, 8, 14800, https://doi.org/10.1038/ncomms14800, 2017.

620 Arvin, L. J., Riebe, C. S., Aciego, S. M., and Blakowski, M. A.: Global patterns of dust and bedrock nutrient
621 supply to montane ecosystems, Sci Adv, 3, eaao1588, https://doi.org/10.1126/sciadv.aao1588, 2017.

622 Bauters, M., Drake, T. W., Wagner, S., Baumgartner, S., Makelele, I. A., Bodé, S., Verheyen, K., Verbeeck, H.,
623 Ewango, C., Cizungu, L., Van Oost, K., and Boeckx, P.: Fire-derived phosphorus fertilization of African tropical
624 forests, Nat Commun, 12, https://doi.org/10.1038/S41467-021-25428-3, 2021.

625 Bradl, H. B.: Adsorption of heavy metal ions on soils and soils constituents, J Colloid Interface Sci, 277, 1–18,
626 https://doi.org/10.1016/J.JCIS.2004.04.005, 2004.

627 Burkhardt, J., Basi, S., Paryar, S., Hunsche, M.: Stomatal penetration by aqueous solutions- an update involving
628 leaf surface particles. New Phytologist, 196, 774-787, 2012.

629 Burkhardt, J., and Eichert, T.: Chapter 4 - Uptake and Release of Elements by Leaves and Other Aerial Plant
630 Parts, in: Marschner's Mineral Nutrition of Higher Plants, 4th ed., edited by: Rengel, Z., Cakmak, I., and White,
631 P. J., Elsevier, London, pp. 71–112, 2022.

632 Chadwick, O. A., Derry, L. A., Vitousek, P. M., Huebert, B. J., and Hedin, L. O.: Changing sources of nutrients
633 during four million years of ecosystem development, Nature, 397, 491–497, https://doi.org/10.1038/17276, 1999.

634 Ciriminna, R., Scurria, A., Tizza, G., and Pagliaro, M.: Volcanic ash as multi-nutrient mineral fertilizer: Science
635 and early applications, JSFA Reports, 2, 528–534, https://doi.org/10.1002/JSF2.87, 2022.

636 Clarkson, D. T. and Hanson, J. B.: The mineral nutrition of higher plants, Ann. Rev. Plant Physiol, 31, 239–98,
637 1980.

638 Dam, T. T. N., Angert, A., Krom, M. D., Bigio, L., Hu, Y., Beyer, K. A., Mayol-Bracero, O. L., Santos-Figueroa,
639 G., Pio, C., and Zhu, M.: X-ray Spectroscopic Quantification of Phosphorus Transformation in Saharan Dust
640 during Trans-Atlantic Dust Transport, Cite This: Environ. Sci. Technol, 55, 12694–12703,
641 https://doi.org/10.1021/acs.est.1c01573, 2021.

642 Eger, A., Almond, P. C., and Condron, L. M.: Phosphorus fertilization by active dust deposition in a super-humid,
643 temperate environment—Soil phosphorus fractionation and accession processes, Global Biogeochem Cycles, 27,
644 108–118, https://doi.org/10.1002/GBC.20019, 2013.

645 Farmer, J. R., Hönisch, B., Haynes, L. L., Kroon, D., Jung, S., Ford, H. L., Raymo, M. E., Jaume-Seguí, M., Bell,
646 D. B., Goldstein, S. L., Pena, L. D., Yehudai, M., and Kim, J.: Deep Atlantic Ocean carbon storage and the rise
647 of 100,000-year glacial cycles, Nature Geoscience,12:5, 12, 355–360, https://doi.org/10.1038/s41561-019-0334-
648 6, 2019.

649 Eichert, T. and Fernández, V.: Chapter 4: Foliar nutrient absorption: principles and prospects, in: Marschner's
650 Mineral Nutrition of Higher Plants, 4th Edn., edited by: Marschner, P., Academic Press, London, UK, pp. 123–
651 150, 2022.

652 Fernández, V., Guzmán, P., Peirce, C.A., McBeath, T.M., Khayet, M., McLaughlin, M.J.: Effect of wheat
653 phosphorus status on leaf surface properties and permeability to foliar-applied phosphorus. Plant Soil 384, 7-20,
654 2014a.Gojon, A., Cassan, O., Bach, L., Lejay, L., and Martin, A.: The decline of plant mineral nutrition under
655 rising CO2: physiological and molecular aspects of a bad deal, Trends Plant Sci, 28, 185–198,
656 https://doi.org/10.1016/J.TPLANTS.2022.09.002, 2023.

657 Goll, D. S., Bauters, M., Zhang, H., Ciais, P., Balkanski, Y., Wang, R., and Verbeeck, H.: Atmospheric
658 phosphorus deposition amplifies carbon sinks in simulations of a tropical forest in Central Africa, New
659 Phytologist, 237, 2054–2068, https://doi.org/10.1111/NPH.18535, 2023.

`

Gross, A., Goren, T., Pio, C., Cardoso, J., Tirosh, O., Todd, M. C., Rosenfeld, D., Weiner, T., Custoio, D., and Angert, A.: Variability in Sources and Concentrations of Saharan Dust Phosphorus over the Atlantic Ocean, Environ Sci Technol Lett, 2, 31–37, https://doi.org/10.1021/ez500399z, 2015.

Gross, A., Palchan, D., Krom, M. D., and Angert, A.: Elemental and isotopic composition of surface soils from key Saharan dust sources, Chem Geol, 442, 54–61, https://doi.org/10.1016/j.chemgeo.2016.09.001, 2016a.

Gross, A., Turner, B. L., Goren, T., Berry, A., and Angert, A.: Tracing the Sources of Atmospheric Phosphorus Deposition to a Tropical Rain Forest in Panama Using Stable Oxygen Isotopes, Environ Sci Technol, 50, 1147–1156, https://doi.org/10.1021/ACS.EST.5B04936, 2016b.

Gross, A., Tiwari, S., Shtein, I., and Erel, R.: Direct foliar uptake of phosphorus from desert dust, New Phytologist, 230, 2213–2225, https://doi.org/10.1111/nph.17344, 2021.

Guieu, C., Dulac, F., Desboeufs, K., Wagener, T., Pulido-Villena, E., Grisoni, J. M., Louis, F., Ridame, C., Blain, S., Brunet, C., Bon Nguyen, E., Tran, S., Labiadh, M., and Dominici, J. M.: Large clean mesocosms and simulated dust deposition: A new methodology to investigate responses of marine oligotrophic ecosystems to atmospheric inputs, Biogeosciences, 7, 2765–2784, https://doi.org/10.5194/BG-7-2765-2010, 2010.

Hinsinger, P.: Bioavailability of soil inorganic P in the rhizosphere as affected by root-induced chemical changes: A review, Plant Soil, 237, 173–195, https://doi.org/10.1023/A:1013351617532/METRICS, 2001.

Jweda, J., Bolge, L., Class, C., and Goldstein, S. L.: High Precision Sr-Nd-Hf-Pb Isotopic Compositions of USGS Reference Material BCR-2, Geostand Geoanal Res, 40, 101–115, https://doi.org/10.1111/j.1751-908X.2015.00342.x, 2016.

Kok, J. F., Adebiyi, A. A., Albani, S., Balkanski, Y., Checa-Garcia, R., Chin, M., Colarco, P. R., Hamilton, D. S., Huang, Y., Ito, A., Klose, M., Li, L., Mahowald, N. M., Miller, R. L., Obiso, V., Pérez García-Pando, C., Rocha-Lima, A., and Wan, J. S.: Contribution of the world's main dust source regions to the global cycle of desert dust, Atmos Chem Phys, 21, 8169–8193, https://doi.org/10.5194/ACP-21-8169-2021, 2021.

Lal, R.: Soil degradation as a reason for inadequate human nutrition, Food Secur, 1, 45–57, https://doi.org/10.1007/S12571-009-0009-Z, 2009.

Lambers, H., Albornoz, F. E., Arruda, A. J., Barker, T., Finnegan, P. M., Gille, C., Gooding, H., Png, K., Ranathunge, K., and Zhong, H.: Nutrient-acquisition strategies, in: A Jewel in the crown of a global biodiversity hotspot. , edited by: Lambers, H., Kwongan Foundation and the Western Australian Naturalists' Club Inc., Perth, 2019.

Lokshin, A., Palchan, D., and Gross, A.: Direct foliar phosphorus uptake from wildfire ash, Biogeosciences, 21, 2355–2365, https://doi.org/10.5194/BG-21-2355-2024, 2024a.

Lokshin, A., Gross, A., Dor, Y. Ben, and Palchan, D.: Rare earth elements as a tool to study the foliar nutrient uptake phenomenon under ambient and elevated atmospheric CO_2 concentration, Science of The Total Environment, 948, 174695, https://doi.org/10.1016/J.SCITOTENV.2024.174695, 2024b.

Loladze, I.: Rising atmospheric CO_2 and human nutrition: toward globally imbalanced plant stoichiometry, Trends Ecol Evol, 17, 457–461, https://doi.org/10.1016/S0169-5347(02)02587-9, 2002.

Loladze, I.: Hidden shift of the ionome of plants exposed to elevated CO_2 depletes minerals at the base of human nutrition, Elife, 2014, https://doi.org/10.7554/ELIFE.02245, 2014.

Longo, A. F., Ingall, E. D., Diaz, J. M., Oakes, M., King, L. E., Nenes, A., Mihalopoulos, N., Violaki, K., Avila, A., and Benitez-Nelson, C. R.: P-NEXFS analysis of aerosol phosphorus delivered to the Mediterranean Sea, Geophys Res Lett, 41, 4043–4049, 2014.

Lowe, N. M.: The global challenge of hidden hunger: perspectives from the field, Proceedings of the Nutrition Society, 80, 283–289, https://doi.org/10.1017/S0029665121000902, 2021.

Marschner, H., Kirkby, E. A., and Engels, C.: Importance of Cycling and Recycling of Mineral Nutrients within Plants for Growth and Development, Botanica Acta, 110, 265–273, https://doi.org/10.1111/J.1438-8677.1997.TB00639.X, 1997.

706   Muhammad, S., Wuyts, K., and Samson, R.: Atmospheric net particle accumulation on 96 plant species with
707   contrasting morphological and anatomical leaf characteristics in a common garden experiment, Atmos Environ,
708   202, 328–344, https://doi.org/10.1016/J.Atmosenv.2019.01.015, 2019.

709   Myers, S. S., Zanobetti, A., Kloog, I., Huybers, P., Leakey, A. D. B., Bloom, A. J., Carlisle, E., Dietterich, L. H.,
710   Fitzgerald, G., Hasegawa, T., Holbrook, N. M., Nelson, R. L., Ottman, M. J., Raboy, V., Sakai, H., Sartor, K. A.,
711   Schwartz, J., Seneweera, S., Tausz, M., and Usui, Y.: Increasing CO2 threatens human nutrition, Nature, 510,
712   139–142, https://doi.org/10.1038/nature13179, 2014.Nakamaru, Y., Nanzyo, M., and Yamasaki, S. I.: Utilization
713   of apatite in fresh volcanic ash by pigeonpea and chickpea, Soil Sci Plant Nutr, 46, 591–600,
714   https://doi.org/10.1080/00380768.2000.10409124, 2000.

715   Okin, G. S., Mahowald, N., Chadwick, O. A., and Artaxo, P.: Impact of desert dust on the biogeochemistry of
716   phosphorus in terrestrial ecosystems, Global Biogeochem Cycles, 18, https://doi.org/10.1029/2003GB002145,
717   2004.

718   Palchan, D., Stein, M., Almogi-Labin, A., Erel, Y., and Goldstein, S. L.: Dust transport and synoptic conditions
719   over the Sahara–Arabia deserts during the MIS6/5 and 2/1 transitions from grain-size, chemical and isotopic
720   properties of Red Sea cores, Earth Planet Sci Lett, 382, 125–139, https://doi.org/10.1016/j.epsl.2013.09.013,
721   2013.

722   Palchan, D., Erel, Y., and Stein, M.: Geochemical characterization of contemporary fine detritus in the Dead Sea
723   watershed, Chem Geol, 494, 30–42, https://doi.org/10.1016/J.Chemgeo.2018.07.013, 2018.

724   Parasuraman, P., Pattnaik, S., and Busi, S.: Chapter 10 - Phyllosphere Microbiome: Functional Importance in
725   Sustainable Agriculture, in: Phytomicrobiome Interactions and Sustainable Agriculture, edited by: Rajarshi, K.
726   and Johnson, I., Elsevier, Amsterdam, pp. 185–207, 2022.

727   Shakir, S., Zaidi, S. S. e. A., de Vries, F. T., and Mansoor, S.: Plant Genetic Networks Shaping Phyllosphere
728   Microbial Community, https://doi.org/10.1016/j.tig.2020.09.010, 1 April 2021.

729   Schonherr, J.: Characterization of aqueous pores in plant cuticles and permeation of ionic solutes. J. Exp. Bot. 57,
730   2471 2491, 2006.

731   Starr, M., Klein, T., and Gross, A.: Direct foliar acquisition of desert dust phosphorus fertilizes forest trees despite
732   reducing photosynthesis, Tree Physiol, 43, 794–804, https://doi.org/10.1093/treephys/tpad012, 2023.

733   St.Clair, S. B. and Lynch, J. P.: The opening of Pandora's Box: climate change impacts on soil fertility and crop
734   nutrition in developing countries, 335, 101–115, https://doi.org/10.1007/s, 2010.

735   Stein, M. and Goldstein, S. L.: From plume head to continental lithosphere in the Arabian-Nubian shield, Nature,
736   382, 773–778, 1996.

737   Stockdale, A., Krom, M. D., Mortimer, R. J. G., Benning, L. G., Carslaw, K. S., Herbert, R. J., Shi, Z.,
738   Myriokefalitakis, S., Kanakidou, M., and Nenes, A.: Understanding the nature of atmospheric acid processing of
739   mineral dusts in supplying bioavailable phosphorus to the oceans, Proceedings of the National Academy of
740   Sciences, 113, 14639–14644, 2016.

741   Tanaka, T., Togashi, S., Kamioka, H., Amakawa, H., Kagami, H., Hamamoto, T., Yuhara, M., Orihashi, Y.,
742   Yoneda, S., Shimizu, H., Kunimaru, T., Takahashi, K., Yanagi, T., Nakano, T., Fujimaki, H., Shinjo, R., Asahara,
743   Y., Tanimizu, M., and Dragusanu, C.: JNdi-1: a neodymium isotopic reference in consistency with LaJolla
744   neodymium, Chem Geol, 168, 279–281, https://doi.org/10.1016/S0009-2541(00)00198-4, 2000.

745   Tiwari, S., Erel, R., and Gross, A.: Chemical processes in receiving soils accelerate solubilisation of phosphorus
746   from desert dust and fire ash, Eur J Soil Sci, 73, https://doi.org/10.1111/EJSS.13270, 2022.

747   Van Langenhove, L., Verryckt, L. T., Bréchet, L., Courtois, E. A., Stahl, C., Hofhansl, F., Bauters, M., Sardans,
748   J., Boeckx, P., Fransen, E., Peñuelas, J., and Janssens, I. A.: Atmospheric deposition of elements and its relevance
749   for nutrient budgets of tropical forests, 149, 175–193, https://doi.org/10.1007/s10533-020-00673-8, 2020.

750   Van Oss, R., Abbo, S., Eshed, R., Sherman, A., Coyne, C. J., Vandemark, G. J., Zhang, H. Bin, and Peleg, Z.:
751   Genetic relationship in cicer Sp. expose evidence for geneflow between the cultigen and its wild progenitor, PLoS
752   One, 10, https://doi.org/10.1371/journal.pone.0139789, 2015.

753   Wasserburg, G. J., Jacobsen, S. B., DePaolo, D. J., McCulloch, M. T., and Wen, T.: Precise determination of
754   Sm/Nd ratios, Sm and Nd isotopic abundances in standard solutions, Geochim Cosmochim Acta, 45, 2311–2323,
755   https://doi.org/10.1016/0016-7037(81)90085-5, 1981.

756   Zhu, C., Kobayashi, K., Loladze, I., Zhu, J., Jiang, Q., Xu, X., Liu, G., Seneweera, S., Ebi, K. L., Drewnowski,
757   A., Fukagawa, N. K., and Ziska, L. H.: Carbon dioxide (CO2) levels this century will alter the protein,
758   micronutrients, and vitamin content of rice grains with potential health consequences for the poorest rice-
759   dependent countries, Sci Adv, 4, https://doi.org/10.1126/Sciadv.aaq1012, 2018.

760

761

762

763

764

765

766

767

`